Impacts of precipitation variability on the dynamics of a dry tropical montane forest

Ulrike Hiltner[1,3,*], Achim Bräuning[1], Aster Gebrekirstos[1,2], Andreas Huth[3,4,5], Rico Fischer[3]

[1]*Institute of Geography, Friedrich-Alexander University Erlangen, Wetterkreuz 15, 91058 Erlangen, Germany*
[2]*World Agroforestry Centre (ICRAF), United Nations Avenue, Gigiri, PO Box 30677, 00100 Nairobi, Kenya*
[3]*Department of Ecological Modelling, Helmholtz Centre for Environmental Research – UFZ, Permoserstr. 15, 04318 Leipzig, Germany*
[4]*Institute of Environmental System Research, University Osnabruck, Barbarastr. 12, 49076 Osnabruck, Germany*
[5]*German Centre for Integrative Biodiversity Research iDiv, University of Leipzig, Deutscher Platz 5e, 04103 Leipzig, Germany*
**Corresponding author. Tel. +49 175 5644675; E-mail address: u.hiltner.uh@gmail.com*

Highlights:

- We analyse the aboveground biomass by simulating forest growth and stand composition.
- We demonstrate the first tree-ring chronology of *Croton macrostachyus.*
- Tree-ring measurements contribute to the parameterisation of a process-based forest growth model.
- Growth simulations combine local climatic changes with forest growth dynamics.
- Precipitation variability leads to clear differences in biomass and forest composition.

Abstract

Ecosystem structures of tropical mountain forests are under threat due to changes in climate and land-use. The dry tropical montane forest of Munessa-Shashemene in south-east Ethiopia is a prominent example of degradation and deforestation in the sub-humid tropics. In recent years an increasing number of precipitation events has been observed, mainly during the short rainy season. Moreover, the recent IPCC Report (2014) envisages an increase in total annual precipitation, accompanied by more frequent extreme weather events (drought, torrential rains) for the Horn of Africa until the end of the 21st century.

To evaluate possible consequences for local forest ecosystems, we applied the process-based, individual-oriented forest simulation model Formix3 to identify the influence of precipitation variability on the forest growth dynamics. We parameterised the model using field observation data including, for the first time, a tree-ring chronology of *Croton macrostachyus*. By using different levels of annual precipitation and intra-annual precipitation patterns, we analysed explicit simulation scenarios focussing on both overall and species-specific aboveground biomass dynamics and tree species composition.

We found that the model reproduces aboveground biomass productivity precisely under current precipitation conditions. Variations in precipitation cause ecological shifts in the conditions for tree growth. Biomass and species richness both increase with mean annual

precipitation, with the effects stabilising over time. Our results emphasise the impact of the duration and frequency of periods of water limitation on forest structure and growth.

Our model has a variety of potential applications including investigation of the impacts of precipitation variability on forest structure and tree species diversity. It is thus a useful tool for extrapolating local growth measurements and succession, and analysing the impact of different management strategies on dry tropical montane forests.

Keywords: forest growth model, Formix3, climate change simulation, dry tropical montane forest, Ethiopia, tree-ring measurement

1. Introduction

Changes in climate are predicted to influence future forest conditions such as forest habitat, composition and productivity (Aber et al., 2001; Shugart et al., 2001; IPCC, 2014). For all practical purposes climate change is confident to drive the migration of tree species that result in changes in the geographic distribution of forest types and new mixtures of species within forests. Mainly, tree species are awaited to move northwards or to higher altitudes (Shugart et al., 2001; Dullinger et al., 2012). Moreover, climate change is probably to influence forest productivity, such as photosynthesis, respiration, litter fall, and biomass allocation, depending on location, tree species, water availability and carbon dioxide enrichment (Huth et al., 1998; Shugart et al., 2001). Slightly higher temperatures, a greater accumulation of CO_2 in the atmosphere, and more soil moisture due to higher precipitation levels accelerate growth rates of species in forest ecosystems (Kirilenko and Sedjo, 2007; Achard, 2009). Vice versa, climate variability may also cause plant productivity to drop. In terms of the stabilisation of the global climate as well as the protection of the biodiversity, especially tropical forests play an important role (Myers et al., 2000; Bonan, 2008). They cover approximately 15% of the Earth's land surface, though, containing up to 40% of the terrestrial carbon and net primary production, and probably more than 40.000 tree species are estimated to grow in them (Page et al., 2009; FAO and JRC, 2012; Silk et al., 2015). Intact forest ecosystems are able to bind huge amounts of carbon in their living biomass as well as to regulate the water cycle through processes of evapotranspiration. As a result they stabilise the global climate (Reifsnyder, 1982; Pan et al., 2011). How tropical forests respond to climate change may strongly affect the rate of accumulation of atmospheric CO_2.

Among tropical forest types there is a high risk potential of losing montane forests of the dry tropics, such as semi-humid regions, under observed and predicted climate changes (Colwell and Rangel, 2010; Dullinger et al., 2012). Tropical dry forests account for the largest proportion, more than 40%, of all tropical forests (Murphy and Lugo, 1986). Varying precipitation distributions in regions with dry periods on the one hand and temperature-dependant shifts in the altitudinal zoning of different mountain forest types on the other hand may endanger in particular these forest types and tree species growing in them. Tree species that have to deal with seasonal droughts are using adaption strategies, such as stomata closure or leaf shedding, leading to plant productivity drops in case of water scarcity (Krepkowski et

al., 2011b). It is therefore of a high priority to quantify the effects of current and future shifts in precipitation distributions on forest growth and composition in dry tropical montane forests. Since the main carbon pools are typically the living aboveground biomass and the dead mass of litter, woody debris and soil organic matter (Gibbs et al., 2007), a precise estimation of aboveground forest biomass is very important.

One prominent example in the sub-humid tropics, where climate changes have been observed (Strobl et al., 2011) and are predicted for the future (IPCC, 2014; Niang et al., 2014) is the dry tropical montane forest of Munessa-Shashemene in south-east Ethiopia. Like many other regions in Ethiopia this forest was concerned by deforestation and degradation for a long period of time, whereas the percentage of natural high forest cover decreased from 16% to only 3% during 1972-2000 (Zeleke and Hurni, 2001; Nyssen et al., 2004; Dessie and Kleman, 2007; Garedew et al., 2009). The current forested area covers approximately 23,000 ha, consisting of a mixture of plantations and highly disturbed remnant natural forest patches (Fritzsche et al., 2007). The vegetation of this remnant natural forest is dominated mostly by the indigenous canopy species *Croton macrostachyus* and *Podocarpus falcatus* with existence of other indigenous tree species (Tesfaye et al., 2010). These two dominant tree species are from different functional types and have an ecological and economic importance for the local people (Bekele-Tesemma, 2007; Tesfaye et al., 2010). To ensure that the Munessa-Shashemene Forest and other natural forest remnants are protected and managed sustainably, we need to broaden our knowledge of dry tropical forest ecosystems and the mechanisms that determine natural forest dynamics, which are currently poorly understood. This applies in particular to possible response patterns related to regional climate change scenarios. In this context we are seeking to answer the following questions:

1. How resilient is the forest stand structure and species composition to variations in annual precipitation?

2. What is the influence of intra-annual precipitation variability on the aboveground biomass production?

To assess the possible ecological effects of changes in precipitation patterns on the succession of the investigated forest stand structure of Munessa-Shashamene, we used the process-based, individual-oriented forest simulation model Formix3 including dynamic soil water and precipitation modules (Huth, 1999; Fischer et al., 2014). We developed appropriate climate change scenarios and simulated long-term and large-scale spatiotemporal dynamics of the forest productivity (aboveground biomass). Since our forest model is sensitive to parameter settings for the individual stem diameter increment, these parameters have to be derived precisely for each tree species by means of multi-year tree-ring dating and dendrometer data. We demonstrate the first tree-ring chronology of *C. macrostachyus* and this chronology was used as one part of the parameterisation to adjust parameter values of the model's stem diameter increment curve. Supplementing this investigation of tree-ring dating, additional multi-year dendrometer data for five indigenous tree species of the Munessa-Shashemene forest (Krepkowski et al., 2011a; 2011b) were used to parameterise their diameter increment

curves as well. Concerning the methodology of combining forest modelling and tree-ring dating in the Formix3 model for the first time, this paper addresses another question on how useful dendrochronological measurements for the parameterisation of the forest model's stem diameter increment curves are.

In the following, the model's simulation outcomes of the two experiments with changing annual levels and intra-annual patterns of precipitation will be presented and discussed in relation to changes in aboveground biomass and stem numbers. Then we test the influence of precipitation variability on the growth dynamics of the dry tropical montane forest in Ethiopia. We simulate several annual precipitation patterns, where a single precipitation scenario is defined by the change in precipitation amount and the change in precipitation frequency. Furthermore, we assess the value of dendrochronological data for the parameterisation of stem diameter increment curves.

2. Materials and Methods

2.1. Study area and forest inventory

The study site is located in the dry tropical mountain forest of Munessa-Shashemene in south-east Ethiopia at an altitude of 2,300m a.s.l. (7°26'N, 38°52'E; Fig. 1 left). The photograph (Fig. 1 right) shows the structure of the natural forest consisting of indigenous tree species of different life-forms like evergreen conifers (*Podocarpus falcatus*), evergreen broad-leafed trees (*Syzygium gineese, Prunus africana, Aningeria adolfi-friedericii, Allophylus abyssinicus, Polyscias fulva, Olea capensis*), and deciduous broadleaved trees (*Croton macrostachyus, Celtis africana*) (Bekele-Tesemma, 2007; Krepkowski et al., 2011a; 2011b).

The annual course of precipitation shows strong seasonal variations, with a long dry season from November to March, a long rainy season from July to October, and a very variable short rainy season from April to June (Fig. 1 left). Climate data registered very close to the study site from 2001-2011 revealed a mean annual precipitation of 1,245mm and a mean annual temperature of 14.9° C. Otherwise, Strobl et al. (2011) suggested that the gap between the short and the long rainy seasons has disappeared (March-May) and the climate has generally become more humid since 2001. This is in line with the recent IPCC Report (2014) and Niang et al. (2014), both of which predict and increase in annual precipitation of 20-30%, accompanied by more frequent extreme weather events, such as drought, heat, and torrential rains, for the Horn of Africa until the end of the 21st century.

The soils at the study site are classified as mollic Nitisols (Fritzsche et al., 2007).

We recorded inventory data from five randomly selected square plots in the natural forest with sides measuring 31.5m in length (total area 0.5ha). To obtain the abundance and tree species diversity, all trees taller than 5m were recorded in these five plots by counting and mapping them (Tab. 1). We measured always the tree height, stem height, crown diameter and diameter at breast height DBH. In total we recorded 223 individual trees belonging to 12 different species. The dominant tree species are *P. falcatus* (shade tolerant, climax species,

emergent layer), *C. macrostachyus* (light demanding, pioneer species, canopy layer), and *C. africana* (shade tolerant, emergent layer). From the measured field data we calculated parameters of abundance, stem's basal area and aboveground biomass. Since these are area-specific data, they were extrapolated to 1ha (Tab. B.4). To describe individual tree growth in the process-based Formix3 forest model, the tree geometric values (e.g. tree height, crown diameter, DBH) were used to derive tree allometric relations for the model's parameterisation (e.g., height-diameter relations, stem diameter increment curves) (Tab. B.2) (Huth, 1999). In addition, wood density values were known from literature (Bekele-Tesemma, 2007; Chave et al., 2009); Appendix B Tab. B.1). Supplementing the DBH measurements, we derived species-specific annual growth rates from 19 electronic point dendrometers (Ecomatik, Germany) for the period 2008-2011. These were installed in the natural forest divided to 6 on *P. falcatus*, 5 on *P. africana*, 5 on *C. africana*, 2 on *S. guineese*, and 1 on *A. adolfi-friedericii*. They were attached to the stems at 1-1.5m height. Daily radial stem changes were registered automatically. Here we define 'increment' as a daily net increase of the stem diameter (Krepkowski et al., 2011b) and summed such increment values up to mean annual diameter increment rates (Fig. C.1-C.7). Additionally, tree-ring analyses of five stem discs of *C. macrostachyus* were derived. These discs were sampled within a distance of half a kilometre from the natural forest during ongoing logging events in 2008.

2.2. The FORMIX3 forest model

The following is an overview of the Formix3 forest gap model and its soil water and precipitation sub models. The forest model description follows the protocols published by (Huth et al., 1998; Huth and Ditzer, 2000) and the detailed sub model descriptions can be found in both cases in (Fischer et al., 2014). Field observation data were used to develop a model parameterisation establishing tree allometric values and aboveground biomass. Detailed lists of the parameters used for the model development of the Munessa-Shashemene Forest are given in Appendix B.

2.2.1. Overview

Gap models simulate forest succession in forest gaps based on the germination, growth and mortality of individual trees (Botkin, 1993; Shugart, 1998; Bugmann, 2001; Scholes et al., 2002). Forest gaps are caused by tree fall. Most of these models were applied to temperate and boreal regions. The Formix3 forest model has been well verified and applied to many tropical forest sites (Ditzer et al., 2000; Huth and Ditzer, 2001; Kammesheidt et al., 2001; 2002; Fischer et al., 2014).

The main processes in the Formix3 forest model are tree growth, competition for space, light and soil water availability, mortality, and regeneration (Huth et al., 1998; Huth and Ditzer, 2000; Fischer et al., 2014). Individual tree growth is based on a carbon balance calculated by modelling eco-physiological processes such as photosynthesis, respiration, biomass allocation and litter fall as well as the eco-hydrological condition expressed by the current soil water content. As a result of competition, current photosynthesis rates vary. Mutual spatial restriction on account of canopy-spreading, mutual shading-effects between canopies calculated as a function of light availability, and water limitation due to a drought-related

reduction factor (depending on precipitation and evapotranspiration) influence the photosynthetic production. Mortality depends on various factors including natural ageing, the self-thinning effect caused by high canopy density representing the competition for light and space, and the creation of gaps due to large and dying trees falling and damaging others. Species-specific regeneration rates remain constant over time. In the model, juvenile trees germinate if adequate light conditions on the forest ground and enough space in lower height classes are available.

The process-based, individual-based forest gap model Formix3 simulates forests stands from 1ha up to several km^2 (in this study 1ha). Each hectare is sectored into patches describing the typical size of tree fall gaps (20m × 20m). These patches obtain an explicit spatial position from the model, while the trees within a patch do not. Each of the 12 tree species in our study site are characterised according to their physiological attributes such as shade tolerance and maximum attainable height (Tab. 1). The tree shape is simplified and described by presupposing a conic stem and a spherical crown. The aboveground biomass is calculated for each tree using allometric relationships between DBH, tree height and crown diameter (Fischer et al., 2014). Fig. 2 illustrates a snapshot of a visualisation of Formix3.

2.2.2. Parameter settings

To provide a reference scenario, the model was first calibrated using a parameterisation reflecting the current stock-takings in the study area. The model parameters based on field data (e.g. tree geometric data, climate data, soil taxonomic data, and light energy intensity) and data from literature (e.g. site quality data, tree physiognomic data). All parameters used in the model for the Munessa-Shashemene Forest site are listed by parameter description, values, units as well as references in Appendix B. A small number of uncertain parameter values (maximum photosynthesis rates, mortality rates, number of seeds) were calibrated against field observation data which were calculated for aboveground biomass, stem numbers and basal area (Huth and Ditzer, 2000).

2.3. Annual growth patterns of *C. macrostachyus*

In this study, tree-ring measurements of *C. macrostachyus* were used to calibrate parameter values of the model's diameter increment curve. The cross-section of the deciduous broad-leafed pioneer species *C. macrostachyus* wood shows small and thick-walled fibres, a diffuse ring-porous structure with large vessels, and wood rays with a width of one or two cell rows (Fig. 3.a; Krepkowski et al., 2013). Growth ring boundaries are marked by slightly thickened fibres, but are sometimes difficult to identify microscopically. Macroscopically visible tangential parenchyma bands provide supplementary markers for growth ring boundaries. Dendrometer data of *C. macrostachyus* indicate only one growing season per year lasting from March until November (Krepkowski et al., 2013). Hence, annual increment rates are identifiable.

In total, five stem discs of *C. macrostachyus* were taken from felled trees in 2008, enabling us to follow their anatomical growth ring boundaries over the complete cross-section. All wood samples were sanded with increasingly higher grits of sanding paper to enhance the visibility

of the growth zones. Repeated moistening with water during the ring-width measurement improved the contrast of the wood structures. From each disc, ring width patterns along four radii were measured with a Lintab-Station (Rinntech) to the accuracy of 0.01mm. After crossdating, the radii of one disc were averaged to a mean curve (Rinn, 2003). After identification and dating of missing rings and intra-annual growth bands, the 20 growth curves of *C. macrostachyus* were correctly dated to the final year 2008. Correspondingly, the chronology of *C. macrostachyus* was obtained by synchronising the five mean curves after a second crossdating check **(**Tab. A.1**).**

As illustrated in Fig. 3.b and Fig. 3.c., a 35-year-long ring-width chronology was established for *C. macrostachyus* from measurements of 20 radii of five stem discs. The mean annual radial growth rates R [cm] were converted into diameter increment D_t [cm] at a specific time t [yr], where R_t is the stem radius at the end of the annual increment, and R_{t-1} is the stem radius at the beginning of the annual increment:

$$D_t = 2 \cdot (R_t - R_{t-1}) \qquad (2).$$

Then, D_t was transferred to the model's parameterisation, defining the species' maximum stem diameter increment $g(D)$ per year, where D [cm] is the current stem diameter. Repeated surveys in the study region are used for calibrating the parameter values c and d of the diameter increment curve (see Table A.2; Armstrong et al., 2011; Fischer et al., 2014):

$$g(D) = d \cdot D \cdot \left(1 - {}^{D}/_{D_{max}}\right) \cdot exp^{(-c \cdot D)} \qquad (3).$$

The curve shape (Fig. 3.d) reflects the typical aging trend of one individual tree in the model simulations, revealing maximal possible growth rates without any competition effects (i.e. for light, water, space) (Fischer et al., 2014). For the modelled stem diameter increment curves of other indigenous tree species see Appendix C.

2.4. Simulation experiments

To assess possible ecological effects of changes in precipitation patterns on the growth dynamics of the investigated forest stand structure, appropriate simulation scenarios were developed. In order to investigate different precipitation scenarios, daily precipitation values were simulated based on field observation data. We simulated one IPCC AR5-based scenario (IPCC, 2014; Niang et al.; 2014) and compared the outcomes quantitatively with a reference scenario (Tab. 2): the reference reflects the natural forest development under typical local climate conditions when logging is disregarded. In this reference scenario 1,245mm precipitation was available per year and the intra-annual precipitation distribution corresponds to the hygric seasonality observed at the study area. Because of seasonal variations and inter-annual variability, the year was divided into seasons (quarters) comparable to the hygric seasons in the Munessa-Shashemene Forest (see Chap 2.1) (Fischer et al., 2014): precipitation events occurred most frequently during the long rainy season (quarter 3), and least frequently during the long dry season in quarter 4 and quarter 1, accompanied by the lowest precipitation levels. The short dry season lasts only six to eight weeks and occurs between the short rainy

season (quarter 2) and the long rainy season (Strobl et al., 2011; Krepkowski et al., 2011a; 2011b). Due to this quarter-year resolution, the short dry season is not considered in the precipitation simulations. Daily potential evapotranspiration was calculated with the modified Turc equation (Turc (1961) in Xu and Singh, 2000), and a drought-related reduction factor was calculated from the soil water module (Fischer et al., 2014) to evaluate water availability for biomass production. The precipitation level controlled the soil water content in the model and depending on soil water content a reduction factor due to water deficit (RW [-]) reduced the photosynthesis rate, of an individual tree resulting in productivity drops of the individuals (Fischer et al., 2014). Assuming drought stress during the long dry season during quarter 1 and quarter 4 in the Munessa-Shashemene Forest due to an observed water scarcity (Fig. 1.a), the drought-related reduction factor in the model is given by 0.92 (Strobl et al., 2011; Krepkowski et al., 2011a; 2011b; Fischer et al., 2014). Consequently, the mean soil water content is reduced by 8% in the reference scenario. To simulate the projections for the Horn of Africa envisaged by the IPCC AR5 (2014) and Niang et al., (2014) we adjusted the model parameters for frequency and amount of precipitation. The seasonal precipitation pattern was varied as follows (Tab. 2): (*i.*) the period between two precipitation events was doubled during the long dry season, resulting in -50% precipitation in quarter 4 and quarter 1; (*ii.*) the amount of rain per event was doubled in the short rainy season and in the long rainy season resulting in +50% precipitation in quarter 2 and quarter 3. In this way, the mean annual precipitation amount in the IPCC AR5-based scenario was increased by 25% to 1,565mm/yr.

Additionally, we analysed in total 33 different precipitation levels by varying the mean annual precipitation from 380 to 2,300mm/yr (steps of changes 10%). These variations were adjusted with the corresponding parameters for either the frequency for precipitation events (SET 1) or for the amount of precipitation per event (SET 2) (Tab. B.5). By doing so, we simulated increasing drought stress and torrential rainfall intensity, both of which we are define as type of disturbance, by either reducing precipitation levels to less than 800mm/yr or increasing them by more than 1,200mm/yr, respectively. In our study, we used the Shannon index *H'* to describe the diversity of tree species taking both species numbers and species abundance into consideration (Spellerberg and Fedor, 2003). A change in *H'* was supposed to measure the effect of precipitation variability on the forest's community structure in different climate change scenarios, where p_i is the proportion of individuals belonging to the ith species in the dataset (Huston, 1994):

$$H' = -\sum_{i=1}^{R} p_i \cdot \ln p_i \qquad (1).$$

Generally, the higher the index, the better the equipartition of species (Huston, 1994).

For the analysis of a mature forest, 1 ha of forest succession was simulated. The simulations started with a treeless (clear) area. The model worked with a monthly time step and a total of 2,000 years were simulated. All calculated output values were averaged over 10 simulation-runs to minimise variances (Bennett et al., 2013). Output values were averaged over the last 1,000 years of simulation to obtain mean values for mean forest attributes. Calculations for the years 1 to 1,000 were excluded from further analyses, based on the assumption that forest

succession must be balanced around a climax state after 1,000 years. Standard deviations were given to measure the deviation from the averages, and to interpret the ecosystem's stability (Leyer and Wesche, 2007).

3. Simulation Results

3.1. Calibration results for the reference scenario

The model outputs for the reference scenario correctly predicted the observed overall aboveground biomass (-4.3%) and species-specific estimates of a mature forest stand for trees with DBH above 10 cm (Fig. 4.a). The latter refers to the dominant tree species characterising the canopy and emergent layers (height > 22m), which are the species 1 to 8 (see Tab. 1). In contrast to that, the model outputs of the understorey tree species' aboveground biomass (height 5-22m) showed slight differences in comparison to the observed aboveground biomass values. However, compared to the dominant tree species, the mean aboveground biomasses of the understorey tree species were insignificant (species 9 to 12; see Tab. 1), contributing only 0.5% to the total of 573t_{ODM}/ha (Tab. B.4).

3.2. Influence of a changing seasonal hydrology on forest growth

Precipitation amounts and length of dry intervals determine soil water content and hence influence tree growth dynamics. This was illustrated in the simulation results by the aboveground biomass balance (Fischer et al., 2014). Fig. 5.a, b shows the temporal development and frequency distributions of undisturbed forest growth in the reference scenario as well as for the IPCC AR5-based scenario.

Under current precipitation conditions (1.252mm/yr) being simulated in the reference scenario, the mean soil water content was 30.5% and the drought-related reduction factor was 0.92. Hence, in the reference scenario tree growth was limited by 8%, which was mainly due to effects of drought stress during the long dry season (quarter 4 and quarter 1, Tab. 2). In this context, the overall aboveground biomass was predicted to be 573t_{ODM}/ha (SD ±19t_{ODM}/ha) (averaged over years 1,000-2,000) (Fig. 5.a, c). The main part of the biomass consisted of the emergent tree species *P. falcatus* (389t_{ODM}/ha, SD ±17t_{ODM}/ha), followed by the pioneer tree species *C. macrostachyus* (94t_{ODM}/ha, SD ±2t_{ODM}/ha) (Fig. 5.e). Except for the small, high-frequent fluctuations, the shape of all curves corresponds to an equilibrium state of a mature forest. The high-frequency fluctuations were caused by individual dying trees.

Even though the mean annual precipitation was increased by an average of 25% in the IPCC AR5-based scenario (precipitation 1,565 mm/yr), the biomass balance is very similar. The forest lost 2.27% of its overall biomass to 560t_{ODM}/ha (averaged over years 1k to 2k) whereas the standard deviation increased to ±32t_{ODM}/ha, which is almost twice as high as under current precipitation conditions (Fig. 5.b, d). Generally, the smaller the standard deviation, the more stable is the ecosystem's biomass balance. The model output variations are mainly due to the simulated intra-annual variations in precipitation pattern in comparison to the reference. The model predicts an increase in mean soil water content by +1.4%, accompanied by a slight

decrease of the drought-related reduction factor by -1%. The most sensitive reaction was subjected to the biomass dynamic of *P. falcatus* as indicated by the higher variability of model outputs (SD ±34t_{ODM}/ha) (Fig. 5.f). The aboveground biomass distributions of the remaining tree species stayed almost unchanged over the time of the simulation.

3.3. Influence of different precipitation levels on forest growth

Overall biomass production increases proportionally with the mean annual precipitation up to approximately 1,500mm/yr (Fig. 6.a). For both investigated scenario sets (SET 1 and SET 2) we observed a strong linear relationship between the amount of mean annual rainfall and the aboveground biomass production (Fig. 6.a: dashed lines). However, at around 1,500mm precipitation per year the growth rates of the forest stand's aboveground biomass reached a maximum of approximately 700t_{ODM}/ha. The diverging trend lines as well as results for scenario SET 1 showed stronger effects on tree growth for changes in the amount per precipitation event rather than for changes in the frequency of precipitation events.

Unexpectedly, the simulated aboveground biomass in the IPCC AR5-based predictions decreased in comparison to current stock-takings (-2.45%) despite an increasing mean annual precipitation amount of 25% (Fig. 6.a). At a precipitation level of 1,500 mm/yr, the overall aboveground biomass is considerably lower (-8.9%) than the potential aboveground biomass (around 675t_{ODM}/ha). This indicates that a more extreme long dry season and hence a more pronounced seasonality has a negative effect on forest growth. However, a smaller standard deviation of the simulated biomass values indicated more stable conditions over time.

The effect of climate change on the forest stand's tree species diversity was measured by a change in the Shannon index *H'* as a function of mean annual precipitation (Fig. 6.b). For both sets of rainfall scenarios (changes in precipitation amount and frequency) *H'* peaks between 800 and 1,200mm rain per year (*H'* 1.15 – 1.21). For the Shannon index at a precipitation level of around 1,500mm/yr, the model's prediction is higher in the IPCC AR5-based scenario. We simulated increasing drought stress and torrential rainfall intensity by either reducing precipitation levels to less than 800mm/yr or increasing them by more than 1,200mm/yr, respectively.

4. Discussion

4.1. Model performance

In this study we applied the Formix3 forest model to simulate dynamics of the dry tropical montane forest of Munessa-Shashemene in south-east Ethiopia. The advantage of this individual-based gap model is that it allows an analysis of different forest types at various spatiotemporal scales varying from individual trees to whole forest ecosystems. Considering that model outputs are sensitive to parameter settings, such as the tree species' stem diameter increment, it is important to derive these parameters accurately.

Here we introduced the dendrochronological methods of tree-ring dating and growth measurement into the Formix3 model. Usually, inventory data from DBH measurements of

only one or two consecutive years are used to assess annual increment rates of tree species and to infer species-specific diameter increment curves (Ditzer, 1999; Huth, 1999; Dislich et al., 2009). However, the tree-ring chronology of *C. macrostachyus* enabled us to implement multi-year growth rates as one part of the parameterisation to calibrate values of the model's stem diameter increment curve (see Fig. 3). The same implementation method was used to determine parameter values from the tree species *C. africana, P. falcatus, A. adolfi-friedericii, P. africana, S. guineese,* which were determined by dendrometer measurements over several years (Krepkowski et al., 2011a; 2011b; Appendix C). Addressing the first key question, we asked whether this implementation has a certain advantage for the model's parameterisation of diameter increment curves.

The identified growth patterns - whether determined by ring-width or dendrometer measurements - are highly accurate and provide long-term estimates of tree growth, enabling us to eliminate model parameter uncertainties. In contrast, only a single DBH tape measurement was available for the understorey species *A. abyssinicus*, *P. fulva*, *V. dainellii*, *O. capensis*, *G. saxifraga*, *D. abyssinica*. In those cases parameter values describing the possible stem diameter increment had to be calibrated. One limitation for implementing tree-ring measurements is the wood anatomical structure of some indigenous tree species with a lack of clear growth-rings (Bräuning et al., 2009; 2010). Species-specific increment rates from diverse tree-ring measurements can already be found in online database files, e.g. at the web site of the National Climatic Data Centre (ncdc.noaa.gov, 2014), which provides access to tree-ring data sets at specific locations.

We compared the model simulation outcomes with field observation data to test the reference scenario. Our results show that the model is able to simulate precisely the aboveground biomass of trees with a DBH of over 10cm on a 1ha area (Fig. 4.a). Although understorey trees and shrubs with a height of over 5m, but a DBH smaller than 10cm are missing in the simulation, the overall biomass predictions were not affected due to the small proportion of aboveground biomass of understorey trees.

Our field observation data on aboveground biomasses on a mature forest patch in the Munessa-Shashemene Forest fit well to another experiment (Tesfaye et al., 2010) that estimated the trees' total aboveground biomass on a one hectare area to be 574$t_{ODM.}$ (Tab. B.4). Reasons for the very slight difference of 0.17% between both values may result from distinct conditions during the site inventories, the fact that the study plots were randomly chosen, and different allometric assumptions.

4.2. Forest responses to precipitation variability

Our main results suggest that the 12 tree species growing in the dry tropical montane forest of Munessa-Shashemene react sensitively to changing precipitation. The main objectives of our sensitivity analysis were species-specific and overall aboveground biomass calculations. Daily rainfall values were simulated in precipitation variation experiments, and varying intra-annual as well as inter-annual precipitation patterns were considered in two

ways. By doing so we gained interesting insights from the forest model simulations which were then incorporated into a “what-if” scenario.

The hygric seasonality for the Munessa-Shashemene Forest site is classified as a bimodal precipitation pattern (Fritzsche et al., 2007). Parameter variations, either in changes of frequency or in the amount of precipitation events, change the drought-related reduction factor for photosynthesis in the model thereby influencing radial stem increment and height growth of competing trees (Fischer et al., 2014). In our study, the reduction of tree growth was predicted to be 8 % under current precipitation conditions (drought-related reduction factor 0.92), because of reduced soil water content occurring mainly during the long dry season.

The outcomes can be divided into two categories: (*i*) assuming that the annual precipitation level exceeds 1,500mm, biomass productivity is only slightly affected and tree species diversity and abundance is low. (*ii*) For annual precipitation levels below 1,500mm the forest stand dynamics will be significantly influenced. Even under current precipitation conditions (reference scenario 1,245mm/yr) tree growth is limited by moisture availability mainly during the long dry season. With increasing drought stress both biomass production and species diversity decrease. To a certain extent, some tree species buffer the effects of water scarcity by adaptation (e.g. stomata closure, leaf shedding). Due to intensifying precipitation rates corresponding to less drought stress, tree growth recovers, resulting in an increase in biomass production. At around 1,500mm precipitation per year, the soil water content in the study area is saturated even during the long dry season.

As biodiversity plays a crucial role in tropical forests, our study considered tree species diversity in relation to different precipitation levels. In comparison to the intermediate disturbance hypothesis IDH (Connell, 1978; Huston, 1994) we assume that higher degrees of stress affect tree species diversity and abundance more strongly. In our study, higher degrees of stress were expressed by more frequent events of drought or torrential rains. Regarding this, the ongoing water limitation during a drought reduces the tree’s photosynthetic production due to the drought-related reduction factor in the model (Fischer et al., 2014). The simulated drought stress reduces, therefore, the aboveground biomass production and the species diversity decreases (Fig. 6). Our study suggests that the convergence to and the exceeding of a physiological growth threshold at 1,500mm precipitation per year restructures interspecific competition. Compared to the IDH theory, tree species diversity at intermediate disturbance levels is then maximised as tree species growing at low as well as at high precipitation levels can coexist at our study site.

The third key question this paper addresses is how intra-annual precipitation variation affects tree growth in the Munessa-Shashemene Forest. Our simulations of a “what-if” scenario based on the recent IPCC AR5 (2014) prediction for the year 2100 confirm that even variability in the intensity of precipitation alone can cause structural changes in the studied forest. Similar results were shown in another precipitation variation experiment based on forest growth simulations in temperate forests (Gutiérrez et al., 2014), where changes in frequency and

intensity of precipitation events were found to have different impacts on forest structure and growth. Our study suggests that the quarterly resolution of parameter values for the frequency and amount of precipitation reveal effects of intra-annual droughts or torrential rains on biomass production and species composition and demonstrate subsequent changes in hydrology, forest structure and dynamics.

Despite a constantly higher annual precipitation (+25%) the simulated overall aboveground biomass production is affected only moderately in comparison to the reference scenario. Consequently, the main driver for the vulnerability of the forest stand is a change in hygric seasonality. The simulation results of the IPCC AR5-based scenario show an extent of stress indicated by higher year-to-year variations in the aboveground biomass (SD +68%; Fig. 5). This implies a strong influence of the intra-annual distribution of precipitation on tree growth, whereas the most sensitive growth reactions are shown by the emergent tree species *P. falcatus*. Additionally, a higher frequency of drought events during the long dry season (+50%) has stronger effects on tree growth than higher precipitation amounts during the long rainy season (+50%). Finally, compared to the modelled Shannon index at a precipitation level around 1,500mm/yr, the model prediction is higher in the IPCC AR5-based scenario.

4.3. Perspectives

The forest growth model applied here is a promising tool for extrapolating local forest inventories and simulating the dynamics of a dry tropical montane forest. In our study, attempts are being made to link forest growth to precipitation changes, which were predicted for the east African region (IPCC, 2014). In the future, we intend to analyse growth dynamics, forest structure and species richness in the context of both climate change and potential forest management strategies. In the Munessa-Shashemene Forest deforestation is one of the major threats caused by humans. In the context of these ongoing disturbances of the remnant forest patches, the regeneration of indigenous tree species has become a major problem (Tesfaye et al., 2010). There is a danger that the biological diversity may be lost. The Formix3 forest model will help to provide a better understanding of the complex dynamics of the diverse and vulnerable forest ecosystem. Covering simulations of different logging scenarios will allow the development of management strategies that are ecologically sustainable and economically attractive.

Acknowledgements

We gratefully acknowledge the German Research Foundation for funding the project *"Climate response of tree growth in Ethiopia along an altitudinal transect, and implications on local climate and regional atmospheric circulation dynamics"* (BR-1895/15). We thank *Dr. Julia Krepkowski* for her valuable comments and support, as well as the German Academic Exchange Service for funding *Ulrike Hiltner's* field trip.

References

Aber, J., Neilson, R.P., McNulty, S., Lenihan, J.M., Bachelet, D., Drapek, R.J., 2001: Forest processes and global environmental change: Predicting the effects of individual and multiple stressors. BioScience 51 (9), 735-751.

Achard, F., 2009: Vital Forest Graphics. In UNEP/GRID-Ardenal/UNFF, 75 pp. Ardenal, Norway.

Armstrong, A.H., Shugart, H.H., Fatoyinbo, T.E., 2011. Characterization of community composition and forest structure in a Madagascar lowland rainforest. Tropical Conservation Science 4, 428-444.

Bekele-Tesemma, A., 2007. Useful trees of Ethiopia: Identification, propagation and management in 17 agroecological zones. In RELMA-in ICRAF Project, p. -552. World Agroforestry Centre, Nairobi.

Bennett, N.D., Croke, B.F.W., Guariso, G., Guillaume, J.H.A., Hamilton, S.H., Jakeman, A.J., Marsili-Libelli, S., Newham, L.T.H., Norton, J.P., Perrin, C., Pierce, S.A., Robson, B., Seppelt, R., Voinov, A.A., Fath, B.D., Andreassian, V., 2013. Characterising performance of environmental models. Environ. Modell. Softw. 40, 1-20.

Bonan, G.B., 2008: Forests and climate change: Forcings, feedbacks, and the climate benefits of forests. Science 320, 1444-1449.

Botkin, D.B., 1993. Forest dynamics. Oxford University Press, Oxford, New York, 309 pp.

Bräuning, A., Krepkowski, J., Gebrekirstos, A., 2010. Seasonal growth dynamics of different tree species and their climatic control in Munessa Forest, Ethiopia. In: Levanic, T., Gricar, J., Hafner, P., Krajnc, R., Jagodic, S., Gärtner, H., Heinrich, I., Helle, G. (eds.), TRACE - Tree Rings in Archaeology, Climatology and Ecology. Vol. 8: Proceedings of the DENDROSYMPOSIUM 2009, April 16th - 19th 2009, Otocec, Slovenia. GFZ Potsdam, Potsdam, pp. 146-150.

Bräuning, A., Volland-Voigt, F., von Schnakenburg, P., 2009. Wie wachsen Tropenbäume? Jahrringe als Ausdruck von Klimabedingungen und Lebensform. Biol. unserer Zeit 39, 124-132.

Bugmann, H., 2001. A review of forest gap models. Clim. Change 51, 259-305.

Chave, J., Coomes, D., Jansen, S., Lewis, S.L., Swenson, N.G., Zanne, A.E., 2009. Towards a worldwide wood economics spectrum. Ecol. Lett. 12, 351-366.

Colwell R.K., Rangel, T.F., 2010: A stochastic, evolutionary model for range shifts and richness on tropical elevational gradients under Quaternary glacial cycles. Philosopical Transactions of the Royal Society 365, 3695-3707.

Connell, J.H., 1978. Diversity in tropical rain forests and coral reefs. Science 199, 1302-1310.

Dessie, G., Kleman, J., 2007. Pattern and magnitude of deforestation in the south central Rift Valley region of Ethiopia. Mt. Res. Dev. 27, 162-168.

Dislich, C., Günter, S., Homeier, J., Schröder, B., Huth, A., 2009. Simulating forest dynamics of a tropical montane forest in South Ecuador. Erdkunde 63, 347-364.

Ditzer, T., 1999. Struktur und Dynamik natürlicher und bewirtschafteter Dipterocarpaceenwälder: Eine Fallstudie der Modellbildung und Simulation für die Bewirtschaftung natürlicher Resourcen unter Unsicherheit. eds. H. S. H. Seifert, P. L. G. Vlek, & H.-J. Weidelt, p. -359. Universität Gesamthochschule Kassel, Fachbereich Physik, Verlag Erich Goltze Göttingen.

Ditzer, T., Glauner, R., Forster, M., Köhler, P., Huth, A., 2000. The process-based stand growth model Formix 3-Q applied in a GIS environment for growth and yield analysis in a tropical rain forest. Tree Physiol. 20, 367-381.

Dullinger, S., Gattringer, A., Thuiller, W., Moser, D., Zimmermann, N.E., Guisan, A., Willner, W., Plutzar, C., Leitner., M., Mang, T., Caccianiga, M., Drinböck, T., Ertl, S., Fischer, A., Lenoir, J., Svenning, J.-C., Psomas, A., Schmatz, D.R., Silc, U., Vittoz, P.,

Hülber, K., 2012: Extinction debt of high-mountain plants under twenty-first-century climate change. Nature Climate Change 2, 619-622.

FAO and JRC, 2012: Global forest land-use change 1990-2005, by Lindquist, E.J., D'Annunzio, R., Gerrand, A., MacDicken, A., Achard, F., Beuchle, R., Brink, A., Eva, H.D., Mayaux, P., San-Miguel-Ayanz, J., Stibig, H.-J. FAO Forestry Paper No. 169. Food and Agriculture Organization of the United Nations and European Commission Joint Research Centre, Rome, FAO.

Fischer, R., Armstrong, A., Shugart, H.H., Huth, A., 2014. Simulating the impacts of reduced rainfall on carbon stocks and net ecosystem exchange in a tropical forest. Environ. Modell. Softw. 52, 200-206.

Fritzsche, F., Zech, W., Guggenberger, G., 2007. Soils of the Main Ethiopian Rift Valley escarpment: A transect study. Catena 70, 209-219.

Garedew, E., Sandewall, M., Söderberg, U., Campbell, B.M., 2009. Land-use and land-cover dynamics in the central Rift Valley of Ethiopia. Environ. Manage. 44, 683-694.

Gibbs, H. K., Brown, S., Niles, J. O., Foley, J. A. (2007): Monitoring and estimating tropical forest carbon stocks: Making REDD a reality. Environmental Research Letters 2, 1−13.

Gutiérrez, A.G., Armesto, J.J., Díaz, M.F., Huth, A., 2014. Increased drought impacts on temperate rainforests from southern South America: Results of a process-based, dynamic forest model. PLoS ONE 9, e103226.

Huston, M.A., 1994. Biological diversity. Cambridge University Press, Cambridge, 681 pp.

Huth, A., 1999. Modellierung des Wachstums und der Nutzung von tropischem Regenwald. p. -308. Berlin.

Huth, A., Ditzer, T., 2000. Simulation of the growth of a lowland Dipterocarp rain forest with FORMIX3. Ecol. Modell. 134, 1-25.

Huth, A., Ditzer, T., 2001. Long-term impacts of logging in a tropical rain forest - a simulation study. Forest Ecol. Manag. 142, 33-51.

Huth, A., Ditzer, T., Bossel, H., 1998. The rain forest growth model FORMIX3. Verlag Erich Goltze, Göttingen, 182 pp.

IPCC, 2014: Climate Change 2014: Impacts, Adaptation, and Vulnerability. Part A: Global and Sectoral Aspects. Contribution of Working Group II to the Fifth Assessment Report of the Intergovernmental Panel on Climate Change[Field, C.B., V.R. Barros, D.J. Dokken, K.J. Mach, M.D. Mastrandrea, T.E. Bilir, M. Chatterjee, K.L. Ebi, Y.O. Estrada, R.C. Genova, B. Girma, E.S. Kissel, A.N. Levy, S. MacCracken, P.R. Mastrandrea, and L.L. White (eds.)]. Cambridge University Press, Cambridge, United Kingdom and New York, NY, USA, 1132 pp.

Kammesheidt, L., Köhler, P., Huth, A., 2001. Sustainable timber harvesting in Venezuela: a modelling approach. J. Appl. Ecol. 38, 756-770.

Kammesheidt, L., Köhler, P., Huth, A., 2002. Simulating logging scenarios in secondary forest embedded in a fragmented neotropical landscape. Forest Ecol. Manag. 170, 89-105.

Kirilenko, A.P., Sedjo, R.A., 2007: Climate change impacts on forestry. PNAS 104 (50), 19697-19702.

Krepkowski, J., Bräuning, A., Gebrekirstos, A., 2011a. Growth dynamics of *Podocarpus falcatus*. In: Maaten-Theunissen, M., Spiecker, H., Gärtner, H., Helle, G., Heinrich, I. (eds.), TRACE - Tree rings in archaeology, climatology and ecology. Vol. 9. GFZ, Potsdam, pp. 6-12.

Strobl, S., 2011b. Cambial growth dynamics and climatic control of different tree life forms in tropical mountain forest in Ethiopia. Trees-Structure and Function 25, 59-70.

Krepkowski, J., Gebrekirstos, A., Shibistova, O., Bräuning, A., 2013. Stable carbon isotope labeling reveals different carry-over effects between functional types of tropical trees in an Ethiopian mountain forest. New Phytol. 199, 431-440.

Leyer, I., Wesche, K., 2007. Multivariate Statistik in der Ökologie. Springer, Berlin Heidelberg, 232 pp.

Murphy, P.G., Lugo, A.E., 1986: Ecology of tropical dry forest. Ann. Rev. Ecol. Syst. 17, 67-88.

Myers, N., Mittermeier, R.A., Mittermeier, C.G., da Fonseca, G.A.B., Kent, J., 2000. Biodiversity hotspots for conservation priorities. Nature 403, 853-858.

NCDC.NOAA.GOV (2014) Contributors of the International Tree-Ring Data Bank, IGBP PAGES/World Data Center for Paleoclimatology, NOAA/NCDC Paleoclimatology Program, Boulder, Colorado, USA. Internet: www.ncdc.noaa.gov/data-access/paleoclimatology-data/datasets/tree-ring (09.10.2014).

Niang, I., Ruppel, O. C., Abdrabo, M. A., Essel, A., Lennard, C., Padgham, J., Urquhart, P., 2014. Africa. In: Barros, V.R., Field, C.B., Dokken, D.J., Mastrandrea, M.D., Mach, K.J., Bilir, T.E., Chatterjee, M., Ebi, K.L., Estrada, Y.O., Genova, R.C., Girma, B., Kissel, E.S., Levy, A.N., MacCracken, S., Mastrandrea, P.R., White, L.L. (eds.), Climate change 2014: Impacts, adaptation, and vulnerability. Part B: Regional aspects. Contribution of Working Group II to the Fifth Assessment Report of the Intergovernmental Panel on Climate Change. Cambridge University Press, Cambridge, UK, and New York, USA, pp. 1199-1265.

Nyssen, J., Poesen, J., Moeyersons, J., Deckers, J., Haile, M., Lang, A., 2004. Human impact on the environment in the Ethiopian and Eritrean highlands - a state of the art. Earth Sci. Rev. 64, 273-320.

Pan, Y.D., Birdsey, R.A., Fang, J.Y., Houghton, R., Kauppi, P.E., Kurz, W.A., Phillips, O.L., Shvidenko, A., Lewis, S.L., Canadell, J.G., Ciais, P., Jackson, R.B., Pacala, S.W., McGuire, A.D., Piao, S.L., Rautiainen, A., Sitch, S., Hayes, D., 2011. A large and persistent carbon sink in the world's forests. Science 333, 988-993.

Page, S. E., Hoscilo, A., Langner, A., Tansey, K., Siegert, F., Limin, S., et al. (2009). Chapter 9: Tropical peatland fires in Southeast Asia. In M. A. Cochrane (Ed.), Tropical fire ecology: Climate change, land use, and ecosystems dynamics. Berlin: Springer-Praxis, pp. 263−287.

Reifsnyder, W.E., 1982: The role of forests in the global and regional water and energy balances. World Meteorological Organization, GAgM Report No. 8, 33 pp.

Rinn, F., 2003. TSAP-Win. Software for tree-ring measurement, analysis and presentation. Rinntech, Heidelberg.

Scholes, R.J., Dowty, P.R., Caylor, K., Parsons, D.A.B., Frost, P.G.H., Shugart, H.H., 2002. Trends in savanna structure and composition along an aridity gradient in the Kalahari. J. Veg. Sci. 13, 419-428.

Shugart, H.H., 1998. Terrestrial ecosystems in changing environments. Cambridge University Press, Cambridge, 537 pp.

Shugart, H., Sedjo, R., Sohngen, B., 2001: Forests and global climate change. Potential impacts of U.S. forest resources. In PEW Research Center on Global Climate Change, Washington D.C., USA. 64 pp.

Silk, J.W.F., Arroyo-Rodríguez, V., Aiba, S.-I., Alvarez-Loayza, P., Alves, L.F., et al., 2015: An estimate of the number of tropical tree species. PNAS 112 (24), 7472-7477.

Spellerberg, I.F., Fedor, P.J., 2003. A tribute to Claude Shannon (1916-2001) and a plea for more rigorous use of species richness, species diversity and the 'Shannon-Wiener' Index. Global Ecol. Biogeogr. 12, 177-179.

Strobl, S., Fetene, M., Beck, E.H., 2011. Analysis of the "shelter tree-effect" of natural and exotic forest canopies on the growth of young *Podocarpus falcatus* trees in southern Ethiopia. Trees-Structure and Function 25, 769-783.

Tesfaye, G., Teketay, D., Fetene, M., Beck, E., 2010. Regeneration of seven indigenous tree species in a dry Afromontane forest, southern Ethiopia. Flora 205, 135-143.

Zeleke, G., Hurni, H., 2001. Implications of land use and land cover dynamics for mountain resource degradation in the Northwestern Ethiopian Highlands. Mt. Res. Dev. 21, 184-191.

Xu, C.-Y., Singh, V.P., 2002: Evaluation and generalization of radiation-based methods for calculating evaporation. Hydrological Processes, 14 (2), 339-349.

Legend list of figures, tables, and appendices

Figures

Fig. 1: (left) Walter-type climate diagram covering the years 2001-2011 for the study site in the Munessa-Shashemene Forest in south-east Ethiopia (7°26'N 38°52'E, 2,300 m a.s.l.) showing semi-humid conditions. (Right) Photograph of the natural tropical montane forest of Munessa-Shashemene.

Fig. 2: Snapshot of a visualisation of Formix3, showing all trees above a threshold DBH ≥ 10 cm on an area of 1 ha. Each colour represents one species. The dominant canopy group consists of the climax species *P. falcatus* which has a potential DBH > 150 cm. The majority of individuals belong to the pioneer species *C. macrostachyus*. Snapshot of a simulation of the stand after 1,000 years.

Fig. 3: Annual growth patterns of *C. macrostachyus*. (a) The wood anatomical structure of the deciduous broad-leafed *C. macrostachyus* depicted in a cross-section with vessels (V), rays (R) and growth-ring boundary (GRB), marked by slightly thickened fibres (Krepkowski et al., 2013). (b) Tree-ring chronology of *C. macrostachyus* showing the mean annual increment rates over 35 years with a 5-year running mean and the mean ring-width. (c) Number of synchronised trees. Mean annual radial growth rates were converted to basal area increment, and transferred to (d) the model's parameterisation, defining the stem diameter increment curve. The curve shape shows the aging trend of an individual tree in the forest model without any competition effects (Formix3).

Fig. 4: Calibration results. Comparison between field observation data and simulation outcomes resulting from the reference scenario, and illustrating the mean values of the aboveground biomass (averaged over years 1,000-2,000).

Fig. 5: Simulation outcomes for the reference scenario and the IPCC AR5-based scenario (IPCC, 2014), showing (a, b) the temporal development of forest growth for the total and species-specific aboveground biomass on a logarithmic scale. The simulations started with a clear area of 1 ha, and are calculated for monthly time steps over 2,000 years. (c, d) The centre panels show frequency distributions for the overall and the emergent tree species *P. falcatus*, and the right panels (e, f) display relative species compositions of each tree species (averaged over years 1,000 to 2,000).

Fig. 6: Influence of changing precipitation amounts on forest growth. (a) The overall aboveground biomass, including standard deviations, of the mature forest as a function of the amount of precipitation per year split into two sets changing either the amount (SET 1) or the frequency (SET 2) of precipitation between 370–2,500mm/yr (averaged over years 1,000 to 2,000; compare Tab. B.5). Values for IPCC AR5-based (red dots) and reference scenarios (green dots) are highlighted and the dashed trend lines are given for both frequency and amount of precipitation. (b) The sensitivity of the 12 tree species to water availability for each scenario was evaluated using the Shannon index for the relative species compositions.

Tables

Tab. 1: Abundance and maximum tree height of the 12 indigenous tree species at the Munessa-Shashemene Forest site. According to the forest inventory, species were classified into three classes of light demand and six classes of potential height (stratification).

Tab. 2: Simulated precipitation distribution for the reference scenario and the IPCC AR5-based scenario showing increased mean annual precipitation. The year was divided into four seasons (quarters of tree month) corresponding to the intra-annual precipitation pattern at the study site for the simulations with the forest model. All model parameters remain constant except for the parameter values describing *frequency of precipitation events* (F in days) and *amount of rain per precipitation event* (A).

Appendix A. Tree-ring measurement of *C. macrostachyus*

From each stem disc, values of radial growth from four radii were measured and crossdated (Rinn, 2003). After identification and dating of missing rings and intra-annual growth bands, the 20 growth patterns of *C. macrostachyus* were reassessed, correctly dated to the final year 2008 and averaged to a mean curve per tree. Correspondingly, the chronology of C. macrostachyus was obtained by synchronizing the five mean curves after a second crossdating test. Results of sign test and t-value indicate the similarity of each tree mean curve to the final chronology.

Tab. A.1: Crossdating of five C. macrostachyus tree-ring curves. To test the mean tree curves' similarities, statistical parameters were calculated exceeding the threshold values: t-value Bailie & Pilcher (TVBP) ≥ 3 and sign test ≥ 60 % (p < 0.01; ***p < 0.001). The curves' final years were dated to 2008; the longest curve describes the growth pattern over 35 years belonging to sample Croton 03.**

Appendix B. Model Parameterisation

In this part of the Appendix parameter descriptions of the Formix3 model parameterisation for the dry tropical montane forest of Munessa-Shashemene in Ethiopia are listed. Additionally, values that were implemented, and adjusted to the specific study site as well as their units are given.

Tab. B.1: FORMIX3 parameter values used for the simulation of the Munessa-Shashemene Forest, Ethiopia. Specific parameters for each tree species (Sp.) are listed.

Tab. B.2: General parameters used for the simulation of the Munessa-Shashemene Forest in Ethiopia are listed for the FORMIX3 model, the soil water module, the precipitation module, and the carbon flux module.

Tab. B.3: FORMIX3 parameter values used for the simulation of the Munessa-Shashemene Forest in Ethiopia, showing the specific parameters for each height layer.

Tab. B.4: Tree allometric data derived from the forest inventory that was conducted at the study site in Munessa-Shashemene Forest, showing species-specific and overall parameter values.

Tab. B.5: Model parameterisation for all precipitation scenarios on different levels of mean annual precipitation, showing two parameter sets (SET 1 and SET 2). Seasonal precipitation variability was simulated for the IPCC AR5-based (IPCC, 2014) scenario that were made for Ethiopia. To compare the simulation results a reference scenario (RSC) was developed. Except for the parameter values describing frequency for precipitation events and amount of rain per precipitation event, the Fomix3 parameterisation remained constant during the simulations. Moreover, simulated values of mean annual precipitation as well as steps of changes in precipitation compared to the RSC (100%) are given.

Appendix C. Stem diameter increment curves

Supplementing the DBH measurements, we derived species-specific annual growth rates from electronic point dendrometer measurements and tree-ring analyses on five stem discs of *C. macrostachyus.* The dendrometer data were available for the period 2008-2011 for *C. africana, P. falcatus, S. guineese, A. adolfi-fridericii,* and *P. africana* (Krepkowski et al. 2010, 2011 a, b, 2012, 2013).

Fig. C.1: Species-specific stem diameter increment curves as a function of stem diameter. The curve shapes show the aging trend of an individual tree in the forest model without any competition effect (Formix3).

Fig. C.2: The model's parameterisation defining the stem diameter increment curve as a function of stem diameter of *Celtis africana* depicted with dendrometer data. The curve shape shows the aging trend of an individual tree in the forest model without any competition effects (Formix3).

Fig. C.3: The model's parameterisation defining the stem diameter increment curve as a function of stem diameter of *Podocarpus falcatus* depicted with dendrometer data. The curve shape shows the aging trend of an individual tree in the forest model without any competition effects (Formix3).

Fig. C.4: The model's parameterisation defining the stem diameter increment curve as a function of stem diameter of *Aningeria adolfi-friedericii* depicted with dendrometer data. The curve shape shows the aging trend of an individual tree in the forest model without any competition effects (Formix3).

Fig. C.5: The model's parameterisation defining the stem diameter increment curve as a function of stem diameter of *Prunus africana* depicted with dendrometer data. The curve shape shows the aging trend of an individual tree in the forest model without any competition effects (Formix3).

Fig. C.6: The model's parameterisation defining the stem diameter increment curve as a function of stem diameter of *Syzygium guineese* depicted with dendrometer data. The curve shape shows the aging trend of an individual tree in the forest model without any competition effects (Formix3).

Fig. C.7: The model's parameterisation defining the stem diameter increment curve as a function of stem diameter of *Croton macrostachyus* depicted with dendrochronological data. The curve shape shows the aging trend of an individual tree in the forest model without any competition effects (Formix3).

Tab. 1:

species ID	*taxonomic name*	light demand	abundance [1/0.5*ha]	max. tree height [m]	stratifi-cation [m]
1	*Celtis africana*	shade tolerant	10	35	33 > 43
2	*Podocarpus falcatus*	shade tolerant	23	48	< 43
3	*Aningeria adolfi-friedericii*	intermediary	6	50	< 43
4	*Prunus africana*	light demanding	21	37	33 > 43
5	*Syzygium guineese*	light demanding	9	37	33 > 43
6	*Allophylus abyssinicus*	intermediary	7	28	22 > 33
7	*Croton macrostachyus*	light demanding	111	32	22 > 33
8	*Polyscias fulva*	light demanding	13	30	22 > 33
9	*Vepris dainellii*	shade tolerant	2	15	12 > 22
10	*Olea capensis*	intermediary	2	10	8 > 12
11	*Galiniera saxifraga*	shade tolerant	5	12	8 > 12
12	*Dovyalis abyssinica*	shade tolerant	14	8	5 > 8
sum			223		

Tab. 2:

intra-annual precipitation pattern		**reference scenario**		**IPCC AR5-based scenario**	
simulated seasonality	**observed seasonality**	**A [mm]**	**F [d]**	**A [mm]**	**F [d]**
quarter 1	long dry	8.2	4.2	8.2	**6.3**
quarter 2	short rain	9.55	1.7	**14.33**	1.7
quarter 3	long rain	11.8	1.11	**17.7**	1.11
quarter 4	long dry	9.6	3	9.6	**4.5**
simulated mean annual precipitation [mm/yr]		1,245		1,565	

Munessa Forest / Ethiopia
7°26'N/38°53'E
2,300 m a.s.l.

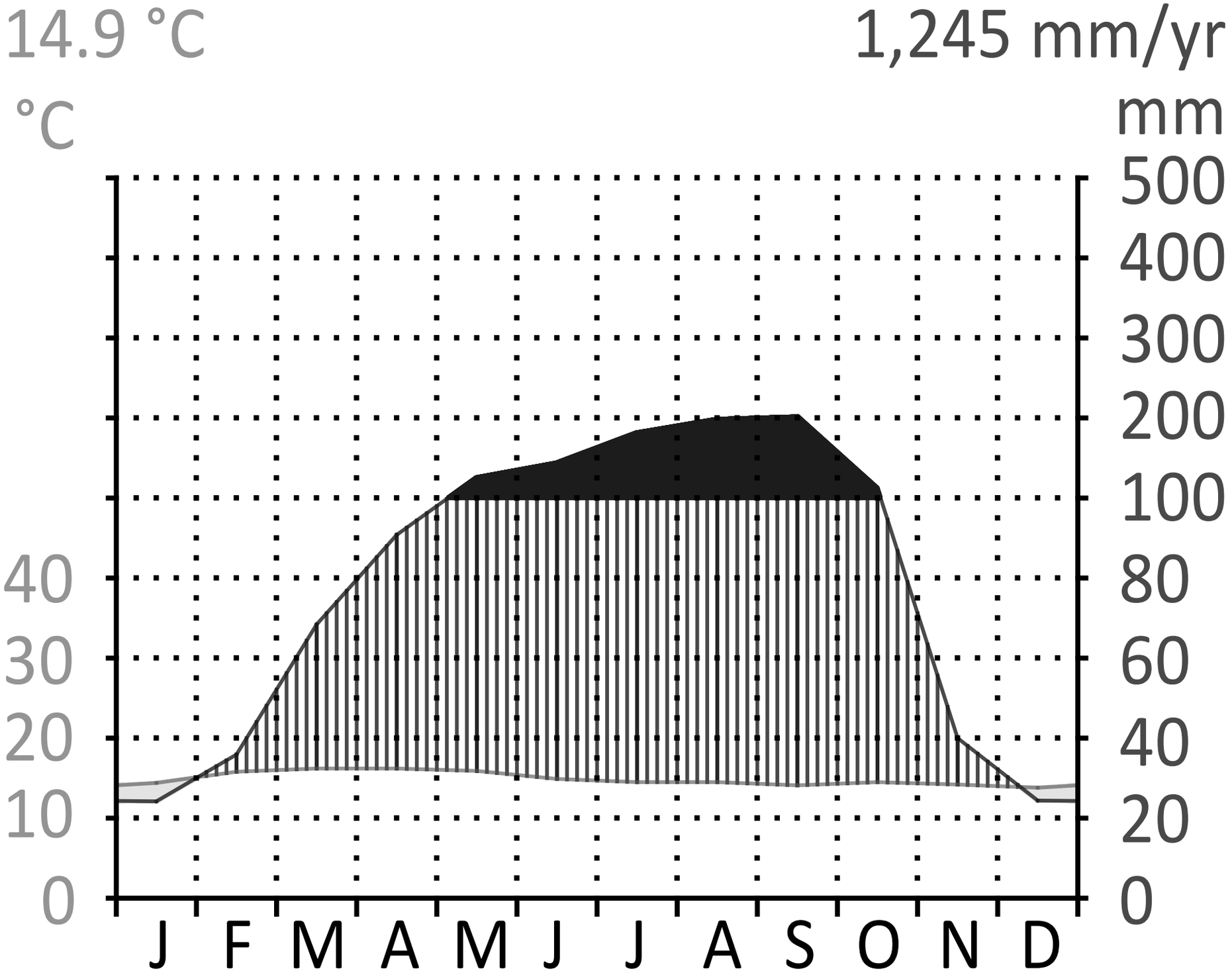

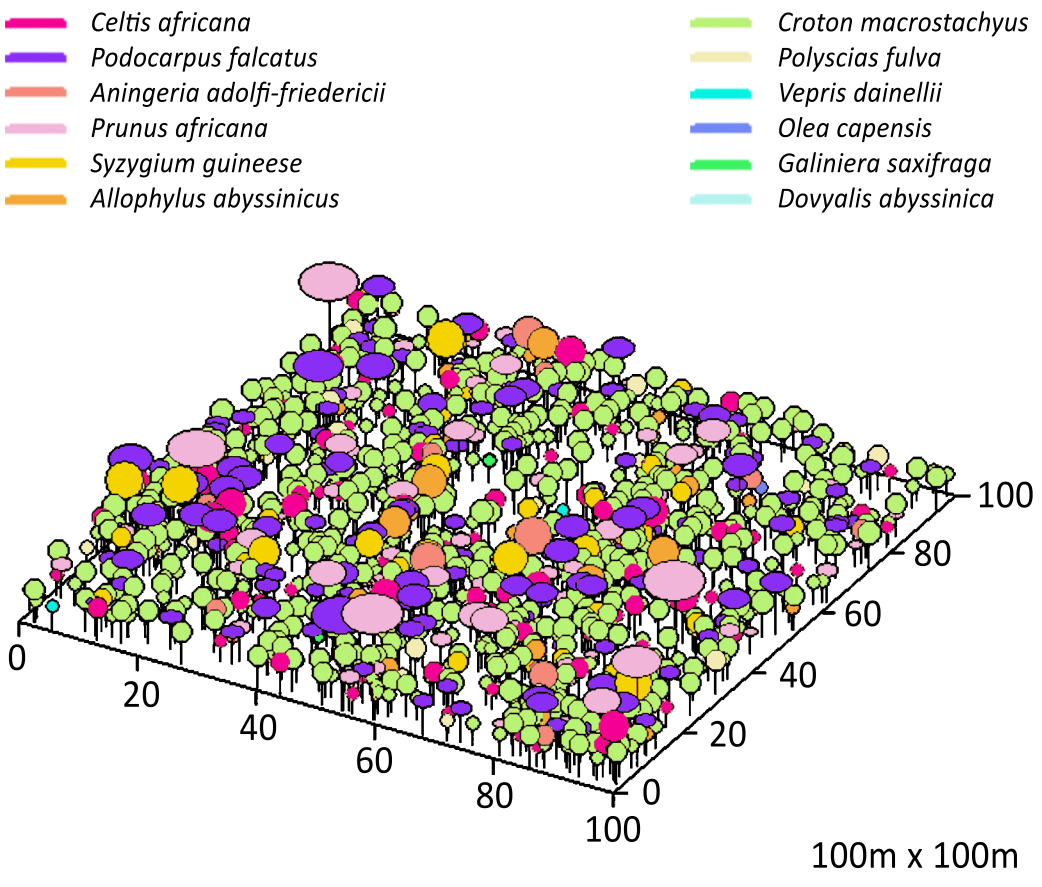
Celtis africana
Podocarpus falcatus
Aningeria adolfi-friedericii
Prunus africana
Syzygium guineese
Allophylus abyssinicus
Croton macrostachyus
Polyscias fulva
Vepris dainellii
Olea capensis
Galiniera saxifraga
Dovyalis abyssinica
0
20
40
60
80
100
0
20
40
60
80
100
100m x 100m

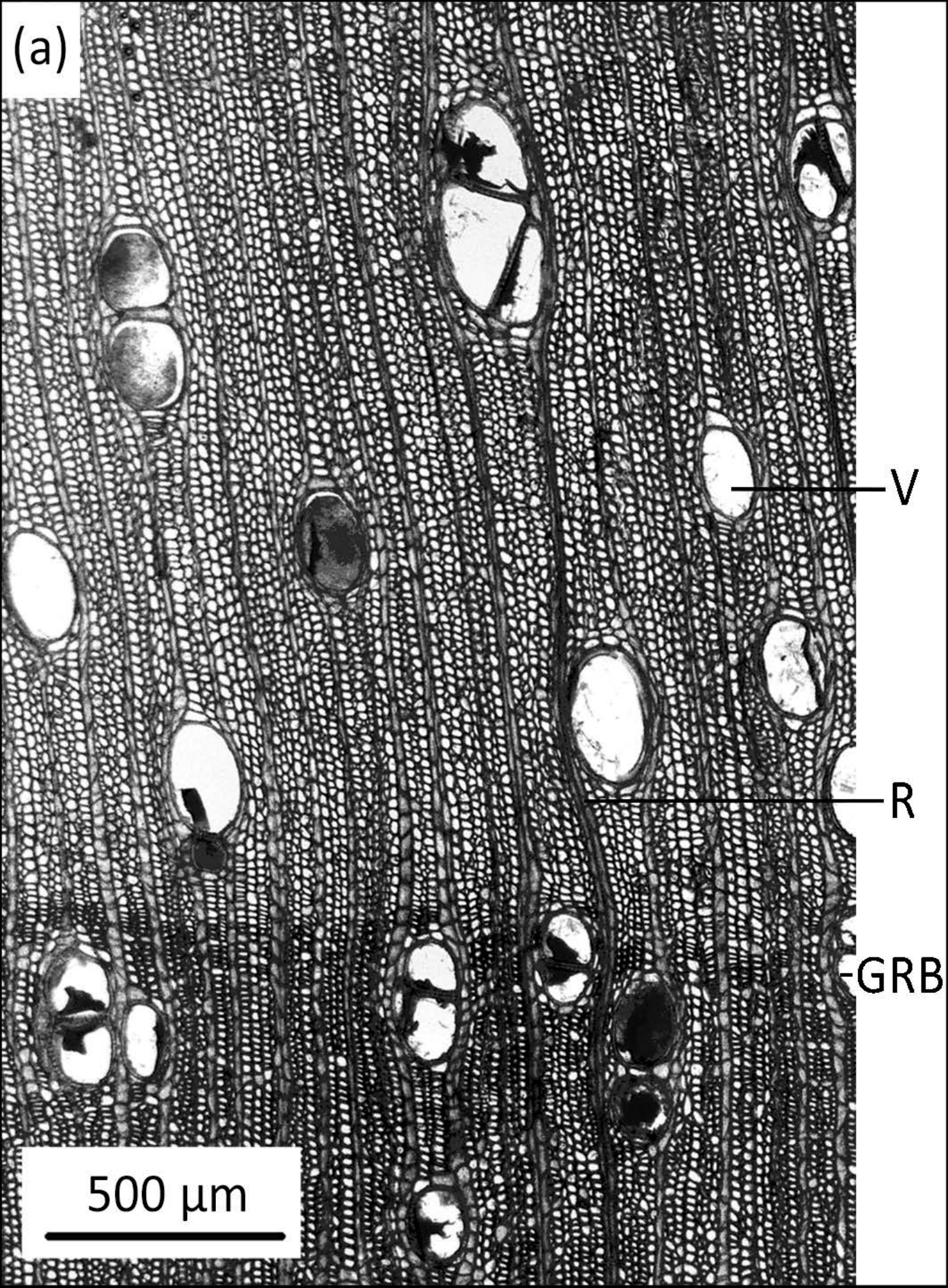
(a)
V
R
GRB
500 µm

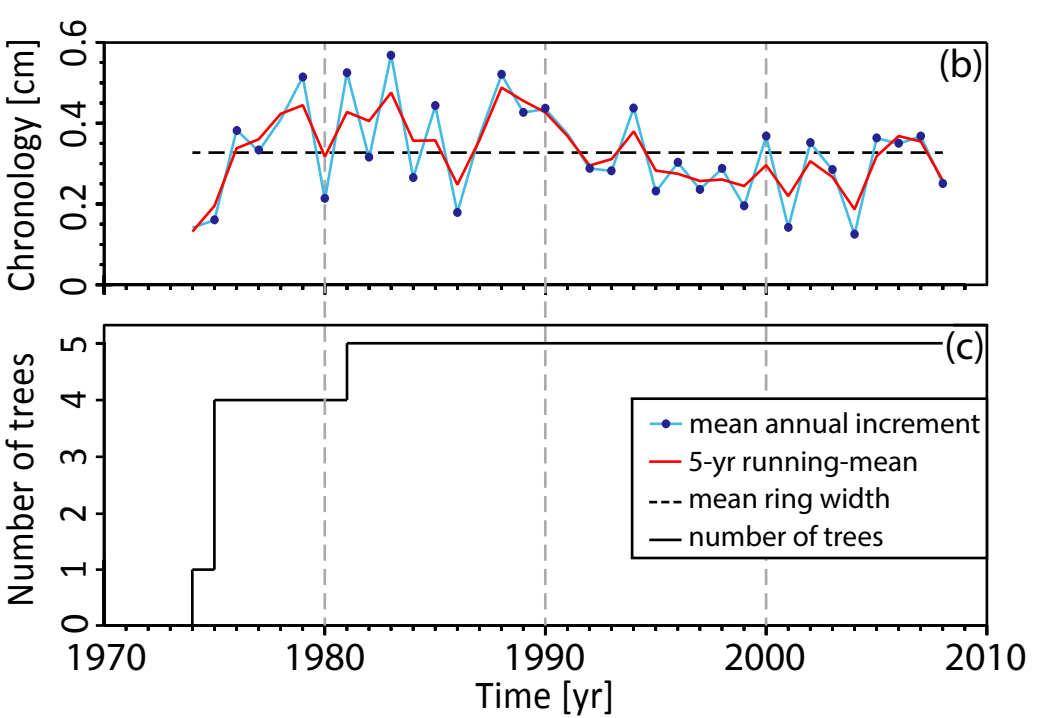
(b)
Chronology [cm]
0
0.2
0.4
0.6
(c)
Number of trees
0
1
2
3
4
5
mean annual increment
5-yr running-mean
mean ring width
number of trees
1970
1980
1990
2000
2010
Time [yr]

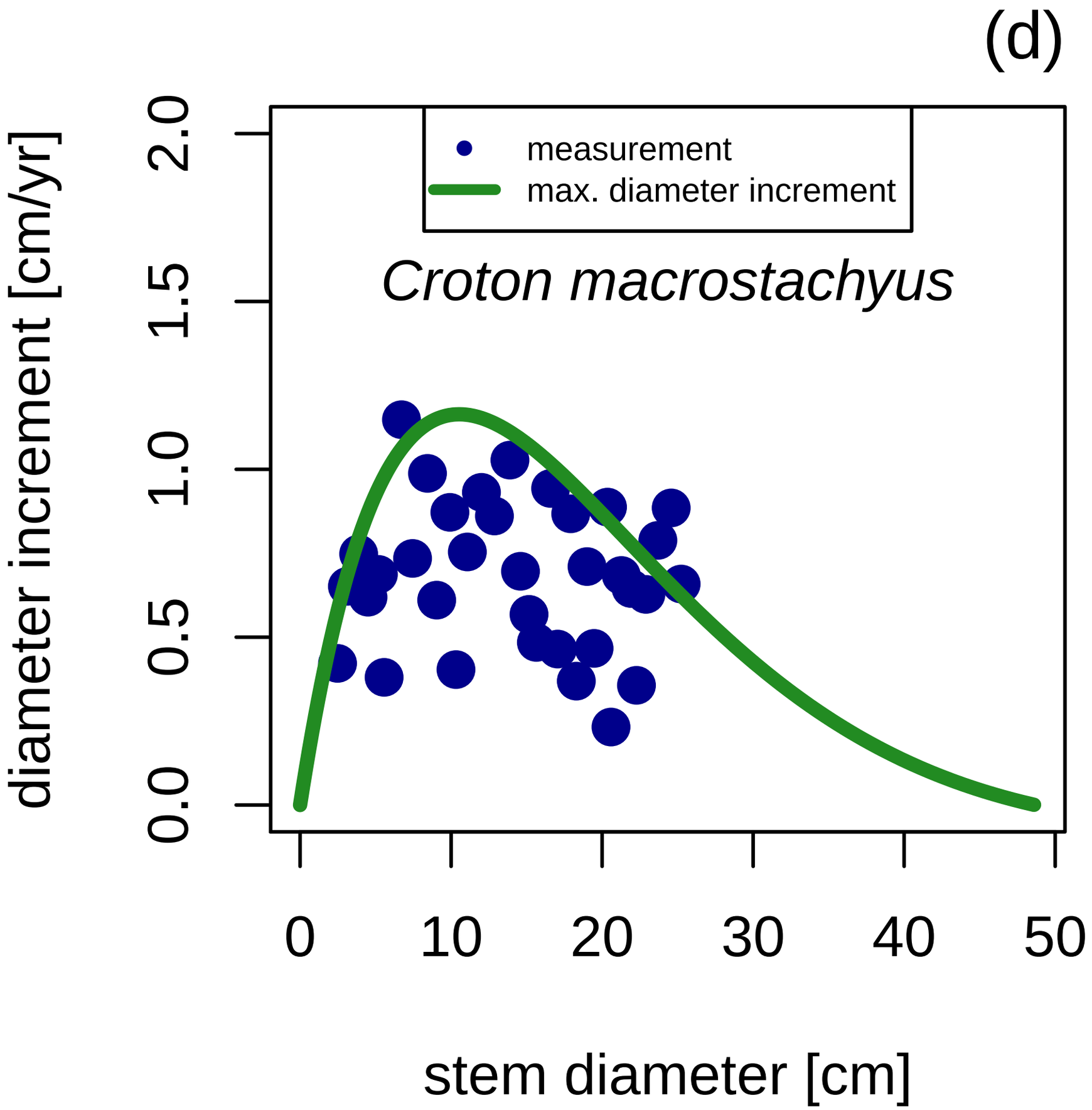
(d)
measurement
max. diameter increment
Croton macrostachyus
diameter increment [cm/yr]
0.0
0.5
1.0
1.5
2.0
0
10
20
30
40
50
stem diameter [cm]

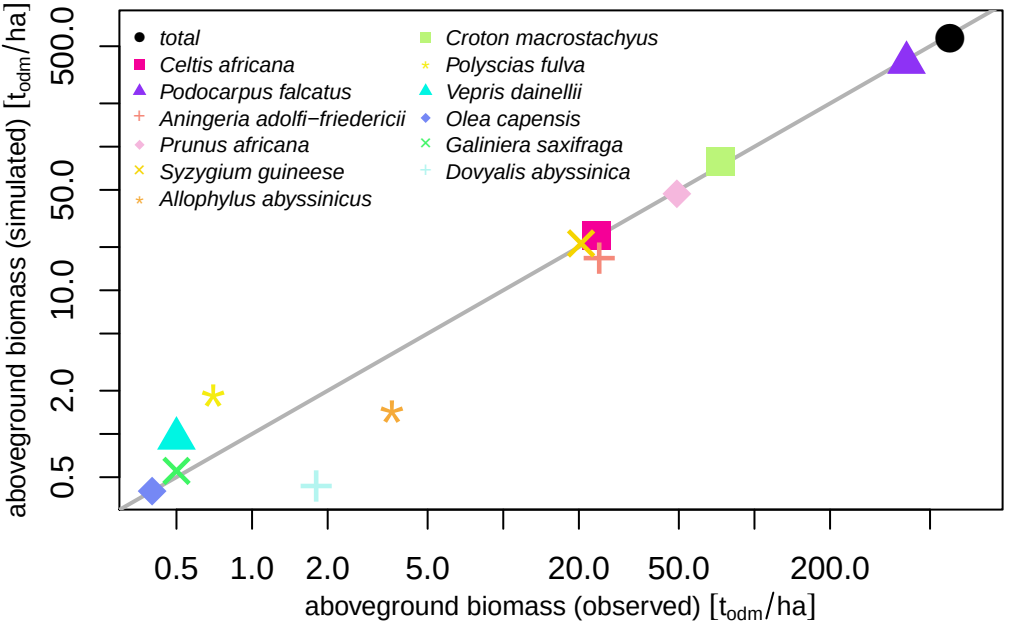
total
Celtis africana
Podocarpus falcatus
Aningeria adolfi−friedericii
Prunus africana
Syzygium guineese
Allophylus abyssinicus
Croton macrostachyus
Polyscias fulva
Vepris dainellii
Olea capensis
Galiniera saxifraga
Dovyalis abyssinica
aboveground biomass (simulated) [t_odm/ha]
0.5
2.0
10.0
50.0
500.0
0.5
1.0
2.0
5.0
20.0
50.0
200.0
aboveground biomass (observed) [t_odm/ha]

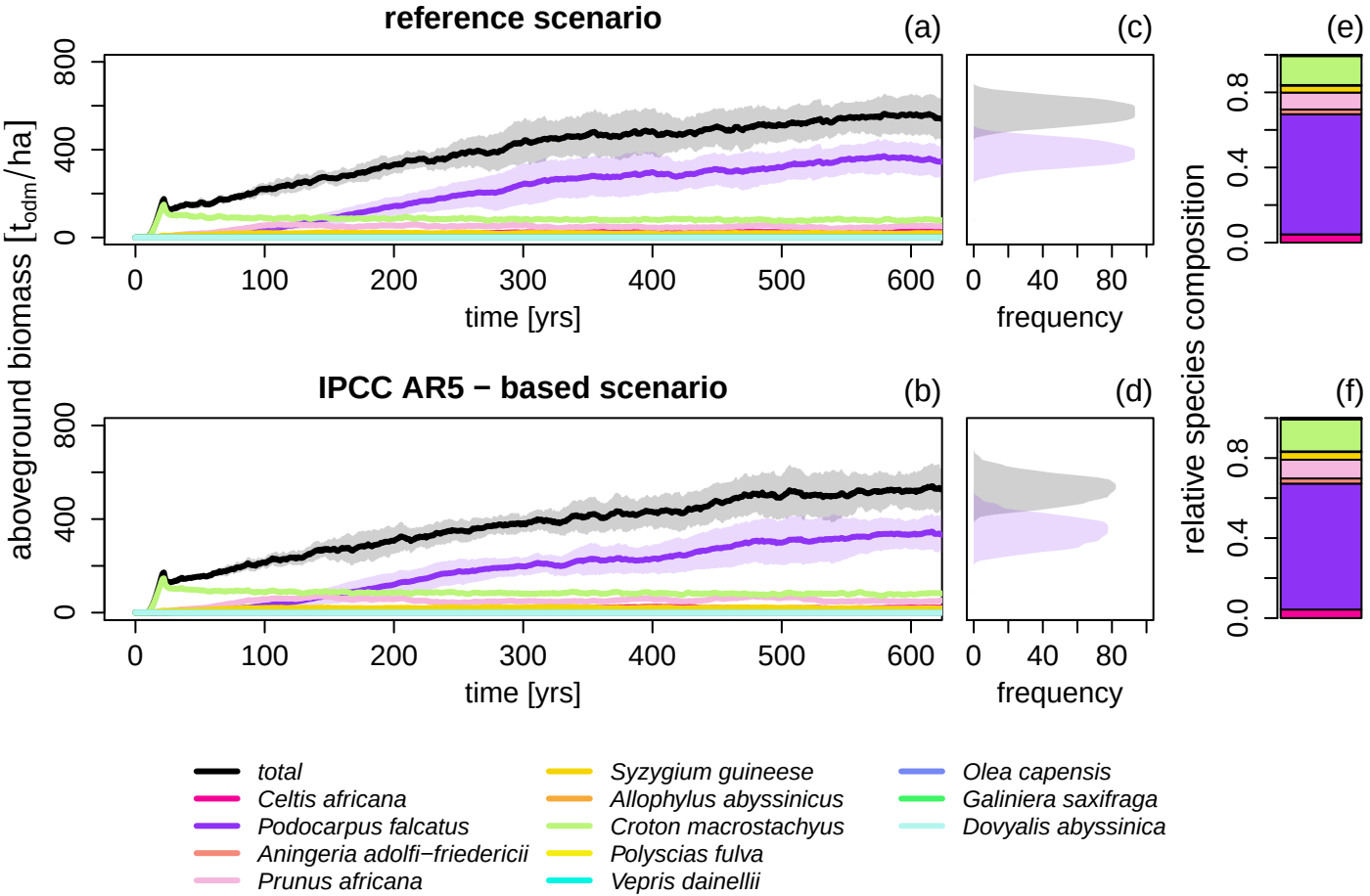
reference scenario
(a)
(c)
(e)
IPCC AR5 − based scenario
(b)
(d)
(f)
aboveground biomass [t_odm/ha]
relative species composition
time [yrs]
frequency
total
Celtis africana
Podocarpus falcatus
Aningeria adolfi−friedericii
Prunus africana
Syzygium guineese
Allophylus abyssinicus
Croton macrostachyus
Polyscias fulva
Vepris dainellii
Olea capensis
Galiniera saxifraga
Dovyalis abyssinica

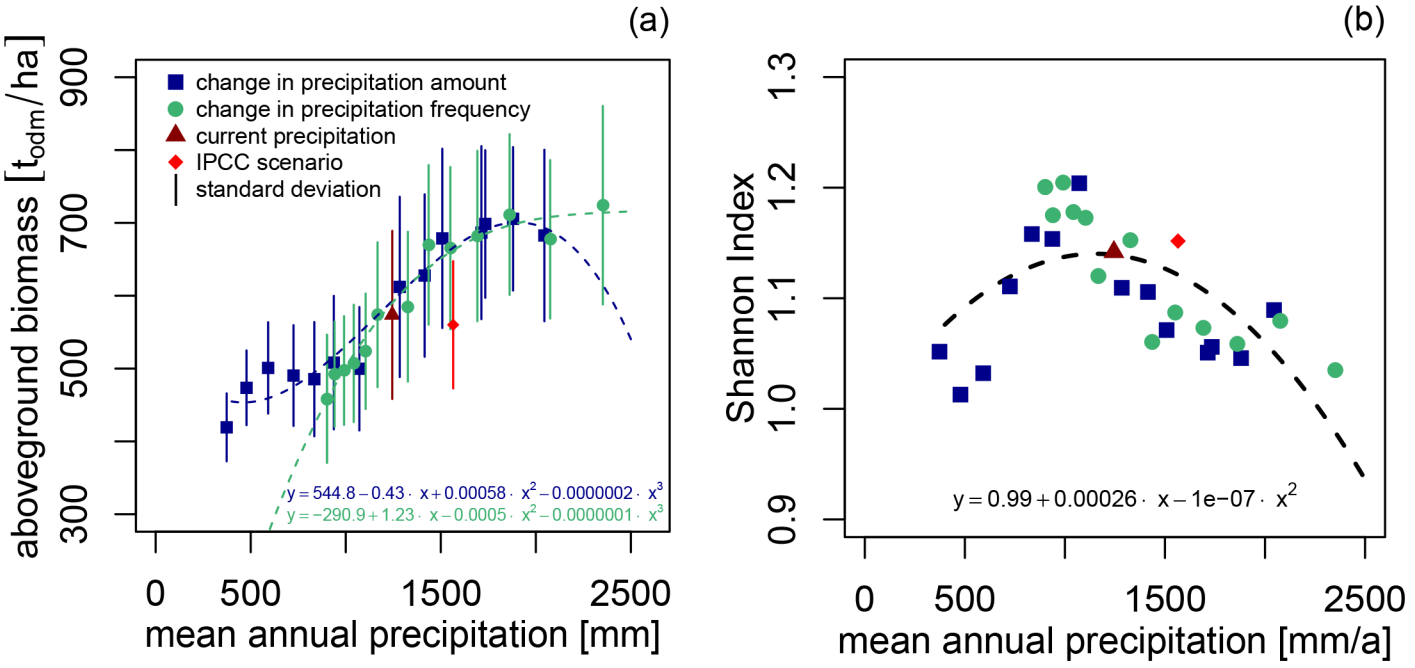
(a)
aboveground biomass [t_{odm}/ha]
300
500
700
900
change in precipitation amount
change in precipitation frequency
current precipitation
IPCC scenario
standard deviation
$y = 544.8 - 0.43 \cdot x + 0.00058 \cdot x^2 - 0.0000002 \cdot x^3$
$y = -290.9 + 1.23 \cdot x - 0.0005 \cdot x^2 - 0.0000001 \cdot x^3$
0
500
1500
2500
mean annual precipitation [mm]
(b)
Shannon Index
0.9
1.0
1.1
1.2
1.3
$y = 0.99 + 0.00026 \cdot x - 1e-07 \cdot x^2$
0
500
1500
2500
mean annual precipitation [mm/a]